JOURNAL OF SOLID STATE CHEMISTRY 54, 179–192 (1984)

Site Selective Spectroscopy and Structural Analysis of Yttria-Doped Zirconias

J. DEXPERT-GHYS, M. FAUCHER, AND P. CARO

Laboratoire des Eléments de Transition dans les Solides CNRS, 1, place A. Briand 92190 Meudon-Bellevue, France

Received January 11, 1984; in revised form April 5, 1984

Yttria-stabilized zirconias $Zr_{1-x}Y_xO_{2-0.5x}$ (tetragonal, cubic fluorite, and cubic -C-Ln_2O_3-type forms) are investigated by spectroscopic methods. Optically active europium ions that partially substitute yttrium ions act as a structural microprobe. Both conventional ultraviolet and dye laser (site-selective) excitation are used. The yttria-stabilized zirconias may be well described by a cationic sublattice in which tetravalent and trivalent cations are statistically distributed. The anionic sublattice accommodates vacancies at random on oxygen positions. These vacancies in turn cause complex oxygen displacements giving rise to what may be described as a "glass of anions."

I. Introduction

By adding heterovalent cations (mainly Ca^{2+} and Y^{3+}) into pure ZrO_2, the high-temperature cubic allotropic form remains stable even at room temperature, as first established by Duwez *et al.* (*1*). This phenomenon greatly improves the mechanical properties of zirconia ceramics by hindering the volume increase associated with the cubic-to-tetragonal-to-monoclinic transformation in pure zirconia. It is also at the origin of the more recent development of partially stabilized zirconia (PSZ) ceramics in ternary systems such as ZrO_2/Y_2O_3/Al_2O_3 (*2*). The stabilization process itself is due to the formation of oxygen vacancies to preserve the charge equilibrium.

These (mobile) defects in turn are responsible for the high ionic conductivity of these materials (*3*), property which has found several applications such as oxygen control devices (*4*) or high-temperature (above 2000 K) furnaces in oxidizing atmosphere (*5*). On the other hand Y_2O_3-stabilized zirconias have been considered as laser host materials (*6*).

Although much work has already been published on yttria-stabilized zirconia there remains unresolved problems concerning the microscopic aspects of the stabilization process (*7*). Most studies are related to their mechanical or physical properties such as electrical conductivity (*8, 9*). On the other hand structural investigations are generally limited to X-ray or neutron diffraction studies (*10*). The cubic fluorite-type structure (noted F) is then usually described by a statistical repartition of Zr^{4+} and Y^{3+} ions in the cationic sublattice together with a random distribution of oxygen vacancies in the anionic sublattice. Evidences for short-range interactions have

0022-4596/84 $3.00

however been put forward. Another cubic "C" (C = rare earth sesquioxide type) solid solution exists in the yttria-rich part of ZrO_2/Y_2O_3 system. Long-range ordering has been observed leading to the $Zr_3Y_4O_{12}$ phase (*11–13*).

In the zirconia-rich part Y^{3+} ions may also enter to some extent the tetragonal (T) or monoclinic (M) phases. As will be discussed below, some points in the phase diagram are still controversial due to the difficulties encountered in reaching true equilibrium conditions.

In this paper we present an optical study of the F, C, and T phases, Eu^{3+} partially substituting Y^{3+} ions and behaving as an optical local microprobe. The systematic interpretation of Eu^{3+} fluorescence spectra on a structural point of view has proven to be very efficient when studying rare earth- or yttrium-mixed oxides systems, especially in the case of Ln^{3+} multisite compounds for which dye laser site-selective excitation is essential (*14*). The same techniques have successfully applied, for example, to rare earth-doped calcium fluorite or calcium oxide crystals (*15, 16*) or to glassy matrices (*17*).

Applications of local probe investigations to ZrO_2/Y_2O_3 are very scarce (see, for example, Refs. (*18–20*)). We prove here that by getting a response from the heterovalent cation (here Eu^{3+} partially substituting Y^{3+}) the optical probe technique gives a new insight in the structural problems linked to short- and long-range ordering.

II. Experimental

Sample preparation. Powdered samples were prepared by coprecipitation starting from zirconium oxichloride, yttrium, and europium oxides (Johnson Matthey 99.99%). Zirconium oxichloride $ZrOCl_2 \cdot nH_2O$ and oxides Y_2O_3 and Eu_2O_3 in appropriate proportions were dissolved in hot concentrated HCl and the mixture of hydroxides precipitated by adding NH_4OH at high temperature (approaching the boiling point). After filtration and washing, the precipitate was fired for 5–6 hr at 1100°C. The water percentage in zirconium oxichloride has been determined by dissolving it in known proportion and then precipitating ZrO_2 in the same experimental conditions as previously detailed. The ZrO_2 weight permitted to deduce the n value in $ZrOCl_2 \cdot nH_2O$. The powders were pressed in thin plates and then fired in a lime-stabilized zirconia heating element at 1750–1800°C during about 20 hr. Cooling down to room temperature was usually achieved by removing the sample from the heating element without further temperature control. However, no modification of the results was observed for slower coolings (several steps of 2 or 3 hr). The starting and final compositions were assumed to be identical. The europium content was chosen between 0.5 and 1% of the whole cationic content (Zr^{4+} + Y^{3+} + Eu^{3+}). In the following Ln stands for (Y + Eu).

A single crystal was grown at the Odeillo solar furnace by Dr. A. Rouanet by slow cooling of a melted mixture of oxides with the initial composition $79ZrO_2/20YO_{1.5}/1EuO_{1.5}$. After cutting by following the (100) faces and polishing a single crystal of about 2 × 1 × 0.2 mm was obtained.

Identification of phases. The phases identified by X-ray diffraction are reported in Table I with their observed cell parameters. Three facts are to be pointed out:

—A single tetragonal (T) stabilized phase is identified for $90ZrO_2/10(Y,Eu)O_{1.5}$. Referring to the ZrO_2/Y_2O_3 phase diagram this does not correspond to the equilibrium state at room temperature but to the high-temperature metastable form which should decompose into F + M (fluorine-type cubic + monoclinic) or M + $Zr_3Y_4O_{12}$ under reversible cooling conditions (see Refs. (*12, 13*)) Gupta *et al.* (*21*) stabilized up to 98% tetragonal phase in monoclinic zirconia.

TABLE I

PHASE IDENTIFICATION AND Eu^{3+} EMISSION CHARACTÉRISTICS IN THE SYSTEM $ZrO_2/Y_2O_3:Eu^{3+}$

Initial composition	Crystallographic data	Type of fluorescence spectrum[a]
99.9 ZrO_2, 0.1 $EuO_{1.5}$	Monoclinic a = 5.147 Å, b = 5.109 Å, c = 5.321 Å, β = 99.3°	See Ref. (*26*)
99.7 ZrO_2, 0.3 $EuO_{1.5}$	Monoclinic a = 5.147 Å, b = 5.109 Å, c = 5.321 Å, β = 99.3°	See Ref. (*26*)
98 ZrO_2, 1.5 $YO_{1.5}$, 0.5 $EuO_{1.5}$	Monoclinic a = 5.147 Å, b = 5.109 Å, c = 5.321 Å, β = 99.3°	See Ref. (*26*)
96 ZrO_2, 3.4 $YO_{1.5}$, 0.6 $EuO_{1.5}$	Tetragonal + monoclinic	II
95 ZrO_2, 4.4 $YO_{1.5}$, 0.6 $EuO_{1.5}$	Tetragonal a = 5.116 Å, c = 5.160 Å + monoclinic	I + II
90 ZrO_2, 9 $YO_{1.5}$, 1 $EuO_{1.5}$	Tetragonal a = 5.120 Å, c = 5.160 Å	I + II
82 ZrO_2, 17 $YO_{1.5}$, 1 $EuO_{1.5}$	Cubic (F) a = 5.144 Å	I + II
75 ZrO_2, 24 $YO_{1.5}$, 1 $EuO_{1.5}$[b]	Cubic (F) a = 5.165 Å	I + II + III
67 ZrO_2, 32 $YO_{1.5}$, 1 $EuO_{1.5}$	Cubic (F) a = 5.180 Å	I + II + III
64 ZrO_2, 35 $YO_{1.5}$, 1 $EuO_{1.5}$	Cubic (F) a = 5.183 Å	I + II + III
50 ZrO_2, 49 $YO_{1.5}$, 1 $EuO_{1.5}$	Cubic (F) a = 5.215 Å	I + II + III
43 ZrO_2, 56 $YO_{1.5}$, 1 $EuO_{1.5}$	Cubic (F) a = 5.237 Å	I + II + III
33 ZrO_2, 65.5 $YO_{1.5}$, 1.5 $EuO_{1.5}$	Cubic (F) a = 5.245 Å + cubic (C) $a \sim$ 10.5 Å	I + II + III
25 ZrO_2, 73.5 $YO_{1.5}$, 1.5 $EuO_{1.5}$	Cubic (F) $a \sim$ 5.25 Å + cubic (C) a = 10.556 Å	III
18 ZrO_2, 80.5 $YO_{1.5}$, 1.5 $EuO_{1.5}$	Cubic (F) $a \sim$ 5.25 Å + cubic (C) a = 10.537 Å	III
11 ZrO_2, 87.5 $YO_{1.5}$, 1.5 $EuO_{1.5}$	Cubic (C) a = 10.585 Å	III
5 ZrO_2, 93.5 $YO_{1.5}$, 1.5 $EuO_{1.5}$	Cubic (C) a = 10.604 Å	III
99.3 $YO_{1.5}$, 0.7 $EuO_{1.5}$	Cubic (C) a = 10.604 Å	III

[a] See Section III in text.
[b] Single crystal.

One may think that a very low proportion of M phase has not been detected in our sample but nevertheless it is very nearly 100% tetragonal.

—A cubic (F) single phase is observed between $82ZrO_2/18(Y,Eu)O_{1.5}$ and $43ZrO_2/57(Y,Eu)O_{1.5}$ and a cubic (C) single phase between $11ZrO_2/89(Y,Eu)O_{1.5}$ and Y_2O_3. A two-phase (F + C) domain lies between these compositions. The changes in unit cell parameters versus Me^{3+} concentration are consistent with a solid solution description. These results agree rather well with previous works (*1, 22*).

—We never observed the already reported $Zr_3Y_4O_{12}$-ordered phase (*11–13*). Even after a 3-week annealing at 1200°C, a sample corresponding to this composition did not show extra diffraction lines when compared with the disordered phases.

Powder data on a ground single crystal showed a F-type phase. The true composition of this sample has been estimated to $75ZrO_2/25(Y,Eu)O_{1.5}$ (see Table I) by comparing the cell parameter a = 5.165 Å with the corresponding values in sintered samples.

These conclusions deduced from X-ray diffraction data are confirmed by electronic diffraction experiments although small crystals of C type are detected at a lower $YO_{1.5}$ content (57%); no reflexion due to the hexagonal $Zr_3Y_4O_{12}$ phase has been identified (*23*).

Spectroscopic measurements. The Eu^{3+} fluorescence is mainly due to transitions

$^5D_{J=0-3} \rightarrow {}^7F_{j=0-4}$. The spectra were recorded at 77 K but it is noteworthy that after excitation to upper levels under ultraviolet light they are basically the same at 300 K. The fluorescence spectra exhibit characteristic features (number, relative intensities, and energetical positions of lines) which reflect the local structural properties nearby Eu^{3+}. If these active ions occupy several crystallographic sites in a given compound, all are excited simultaneously by the ultraviolet incident light and the corresponding fluorescence spectra overlap; the individual spectra are then quite difficult to isolate. The technique of site-selective excitation solves this difficulty. It consists in exciting directly the $^7F_0 \rightarrow {}^5D_0$ transition of Eu^{3+} ions in a given site (each site is related to one $^7F_0 \rightarrow {}^5D_0$ energy value) and then analyzing the particular $^5D_0 \rightarrow {}^7F_{J=1-4}$ fluorescent transitions of that site.

The experimental apparatus is made up of a Spectra Physics 375/376 jet-stream dye laser pumped by a Spectra Physics 164 argon ion laser. The dye is Rhodamine 6G (10^{-3} M in ethylene glycol). The wavelength of the laser beam is continuously tunable from about 5700 to 6500 Å, the linewidth being 0.7 cm^{-1}. All the fluorescence spectra are investigated with a Jarrel-Ash 78460 Czerny-Turner spectrometer (focal length 1 m). Conventional ultraviolet excitation is achieved by an Osram HBO 150-W lamp.

III. Optical Study: Results and Discussion

All the fluorescence lines are characterized by rather large widths. Although an exact measurement is hindered by line overlaps we may evaluate it to more than 50 cm^{-1} at 77 K.

The typical unhomogeneous Eu^{3+} linewidths measured in glassy matrices range between 50 and 100 cm^{-1} and even up to 300 cm^{-1} (*17*) whereas the homogeneous linewidth in the same compounds is about 1–3 cm^{-1} (*25*). Although yttria-stabilized zirconias give rise to diffraction patterns (they are not amorphous materials) the fluorescence of Eu^{3+} embedded in these matrices looks like that of the same ion in a glass.

The unhomogeneous broadening of a fluorescence line brings evidence for the different crystal fields experienced by the Eu^{3+} ions around a mean value, in other words the rare earth immediate environments in stabilized zirconia fluctuate slightly from a given ion to the other.

(*a*) *Emission under ultraviolet excitation: line positions and widths.* In Fig. 1 are reported selected fluorescence spectra of Eu^{3+} in the ZrO_2/Y_2O_3 T, F, and C phases under uv excitation. Corresponding to each composition is noted the nature of phases identified by X-ray diffraction. Almost the same spectrum is observed for the compositions $Zr_{1-x}Ln_xO_{2-0.5x}$ with $x = 0.04$, 0.05, 0.10, and 0.18.

The spectrum characteristic of the T and F phases in this composition range consists in three weakly splitted lines for $^5D_0 \rightarrow {}^7F_1$ and two strongly splitted lines for $^5D_0 \rightarrow {}^7F_2$ (with reference to the corresponding splittings S_1 and S_2 of europium-doped C-type yttrium sesquioxide, we can say that the mean splittings in the actual spectrum are equal to $0.6S_1$ and $1.45S_2$).

Additional lines appear for $x = 0.25$ (single crystal), 0.33, 0.36, 0.50, and 0.57. This new spectrum consists in three and two lines for $^5D_0 \rightarrow {}^7F_1$ and $^5D_0 \rightarrow {}^7F_2$, respectively, but the splitting of the $^7F_1$ manifold is larger than here above ($0.8S_1$) and $^7F_2$ is more contracted ($= S_2$). This spectrum remains nearly the same—with decreasing linewidths—when the Y_2O_3 content increases up to the pure C-type phase ($Y_2O_3 : Eu^{3+}$).

(*b*) *Emission under dye laser excitation.* The Eu^{3+} site selective excitation technique has been applied to our samples. In the $^5D_0 \rightarrow {}^7F_0$ spectral range, site resonances were

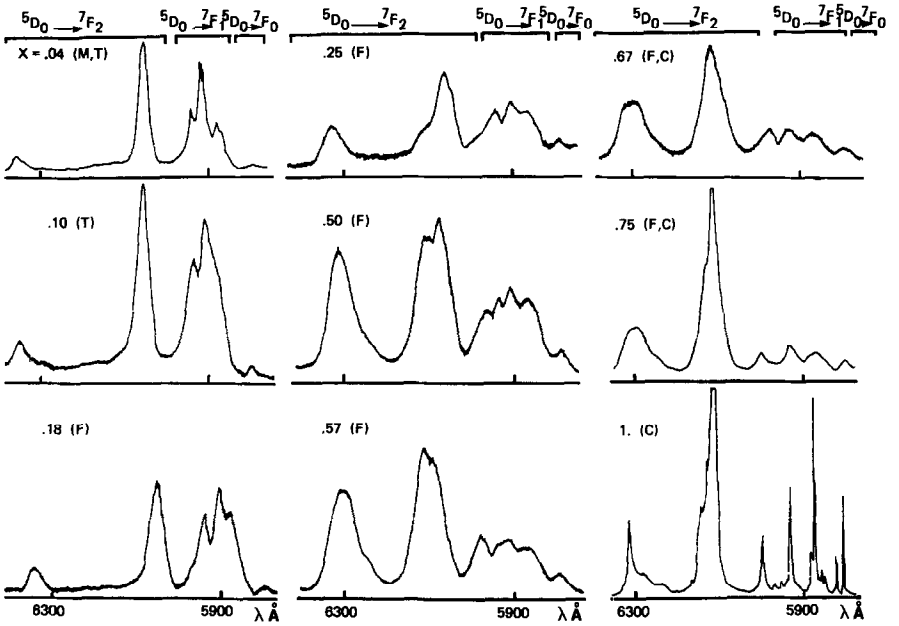

FIG. 1. Fluorescence at 77 K under uv excitation of $Zr_{1-x}Ln_xO_{2-0.5x}$ (Ln = Y + Eu).

systematically sought for by performing tiny displacements of the excitation wavelength followed by a careful scanning of the $^5D_0 \rightarrow {}^7F_2$ region for the fluorescence signal. As for glasses the selective excitation results in fluorescence line narrowing since just a small subset of ions are excited by the laser. Several causes of residual broadening remain in our experiments, for example, site-to-site energy transfer or accidental degeneracy. The first effect might be avoided by time-resolved measurements but the second one would persist in these conditions and even in more selective experiments such as double frequency techniques (*26*). In spite of residual broadening the dye laser excitation brought significant results. We will now describe the selectively excited fluorescence spectra observed for two compositions: $Zr_{0.96}Ln_{0.40}O_{1.98}$ (tetragonal) and $Zr_{0.5}Ln_{0.5}O_{1.75}$ (cubic F).

For the tetragonal form four excitation wavelengths were selected. The four corresponding spectra recorded at 77 K are reported (Fig. 2) and the numerical values are collected in Table II.

For λ_e (excitation) = 5822.5 Å, we obtained a spectrum already observed for

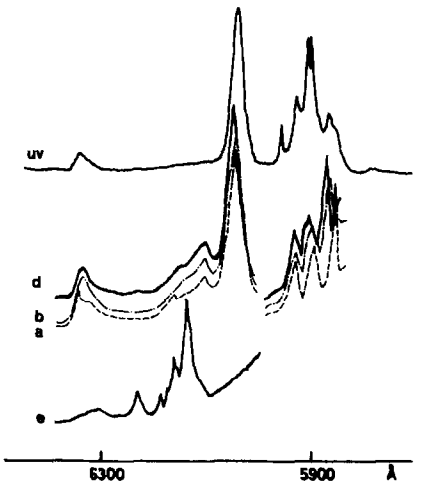

FIG. 2. Fluorescence at 77 K under uv and dye laser excitation of $Zr_{096}Ln_{0.04}O_{1.98}$ (Ln = Y + Eu); see Table II for notations.

TABLE II

NUMERICAL RESULTS OF ULTRAVIOLET AND DYE LASER EXCITATION

$Zr_{0.96}Ln_{0.04}O_{1.98}$					$Zr_{0.50}Ln_{0.50}O_{1.50}$				
Notation (Fig. 2)	Type (see text)	Wavelengths (Å)			Notation (Fig. 3)	Type (see text)	Wavelengths (Å)		
		λ_e	$0 \rightarrow 1$	$0 \rightarrow 2$			λ_e	$0 \rightarrow 1$	$0 \rightarrow 2$
e	Monoclinic	5822.5	5990	6140	a	III	5811.5	5885(III)	6115(III)
				6148				5935(III)	6315(III)
				6171				5965(III)	
				6177	b	II + III	5801.5	5867(II)	6095(II)
				6196				5915(II)	6115(III)
				6244				5935(II + III)	6320(II + III)
				6320				5975(III)	
d	II	5804	5882	6060	c	II + III	5799	5867(II)	6085(II)
			5915	6115				5915(II)	6115(III)
			5944	6350				5935(II + III)	6315(II + III)
								5970(III)	
c	II	5802	5878	6059	d	(I) + II + III	5793	5850(I)	6082(II)
			5915	6120				5867(II)	6115(III)
			5945	6350				5910(II)	6320(II + III)
								5940(II)	
b	II	5800	5875	6055	e	I + II + III	5784.5	5835(I)	6050(I)
			5910	6115				5845(I)	6075(II)
			5950	6350				5880(I)	6115(III)
								5905(II)	6300(I)
								5965(I)	6330(II + III)
a	II	5796	5867	6052	f	I(+ II)	5774.5	5840(I)	6045(I)
			5908	6115				5875(I)	6080(II)
			5941	6330				5900(II)	6300(I)
				6355				5975(I)	6330(II)
uv	II	5795	5870	6055	uv	I + II + III	5795	5855(II)	6080(II)
			5879	6350				5910(II)	6110(III)
			5912					5940(II + III)	
			5918					5965(III)	6315(II + III)
			5940						

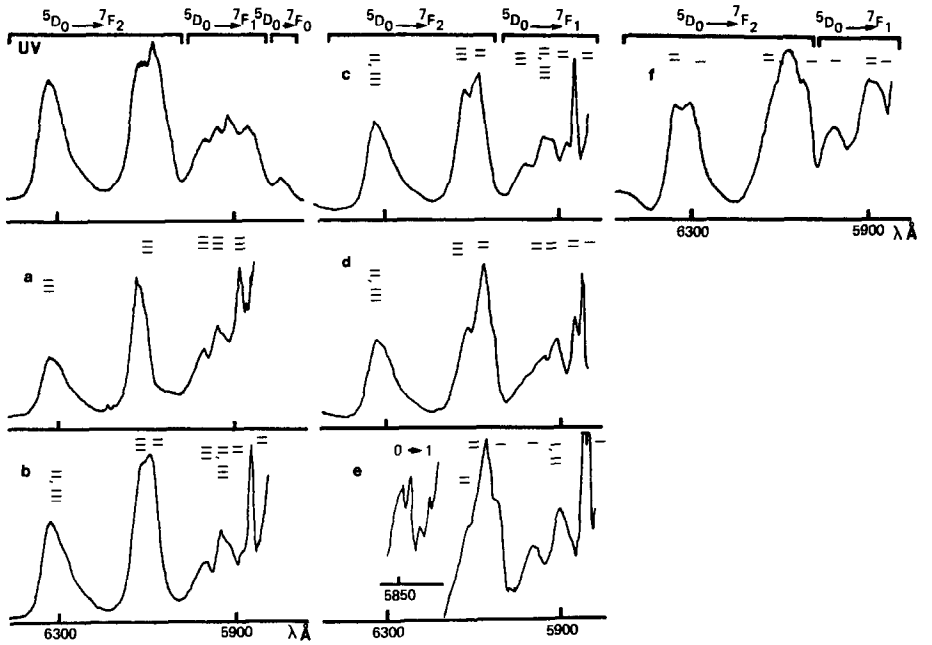

FIG. 3. Fluorescence at 77 K under uv and dye laser excitation of $Zr_{0.50}Ln_{0.50}O_{1.75}$($Ln$ = Y + Eu); see Table II for notations.

Eu^{3+} in monoclinic ZrO_2 (*27*). The monoclinic X-ray diffraction lines are moreover very slightly visible for this sample.

For other excitations only one kind of spectrum was observed with the same overall disposition of lines in each transition but with slight variations of the energy positions.

This spectrum, which we shall denote II, consists in three and two lines for the $0 \rightarrow 1$ and $0 \rightarrow 2$ transitions, respectively. The origin of the additional lines near the strongest $^5D_0 \rightarrow {}^7F_2$ component is not clear since they are invisible on the global uv-excited spectrum. Spectrum II is characterized by small $^7F_1$ and large $^7F_2$ splittings. The $^5D_0 \rightarrow {}^7F_2$ transition displays two lines the more intense of which being probably an unresolved doublet (see spectrum b, Fig. 2).

The uv-excited spectrum being a superposition of the different individual laser-excited spectra, it displays a larger number of lines especially in the $^5D_0 \rightarrow {}^7F_1$ spectral range.

Selectively excited spectra of Eu^{3+} in $Zr_{0.5}Ln_{0.5}O_{1.75}$ are reported in Fig. 3 and the numerical values in Table II. One may observe strong modifications from one excitation wavelength to another. Each spectrum is in fact the sum of several components but the comparison of relative intensities allows to distinguish between three kinds of spectra:

—The spectrum denoted III is characterized by large $^7F_1$ (three lines) and small $^7F_2$ (two lines) splittings (respectively, 248 and 518 cm^{-1}). By comparison with the emission of Eu^{3+} in C–Y_2O_3 (Fig. 1) we may assign III to Eu^{3+} in a C_2-pseudo C_{2v}-hexacoordinated site similar to that of Ln^{3+} in cubic sesquioxide (*28*).

—Spectrum II may be described, on the contrary, by small $^7F_1$ and large $^7F_2$ splittings (209 and 624 cm^{-1}, respectively).

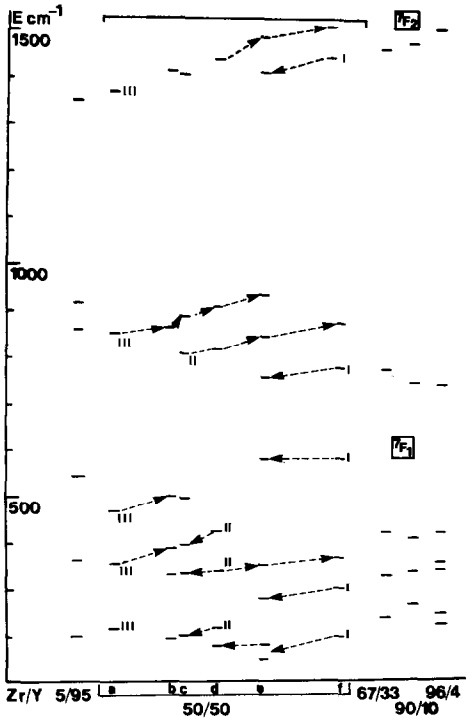

FIG. 4. Eu^{3+} energy levels relative positions from Figs. 1 and 3. Identification of isolated (I,II,III) spectra.

These characteristics had been observed previously for the main component in the $Zr_{0.96}Ln_{0.04}O_{1.98}:Eu^{3+}$ emission.

—Spectrum labeled I is observed for the most energetical excitations and characterized by a very large $^7F_1$ overall splitting (387 cm^{-1}). This last kind of spectra is almost invisible in the uv-excited fluorescence due to wavelengths coincidences with the other two. It was detected by selective excitation in the samples $Zr_{1-x}Ln_xO_{2-0.5x}$ with $x = 0.05$ (T form), 0.25 (single crystal sample, F form), and 0.50 (F form). For $\lambda_e = 5784.5$ Å (Fig. 3e) the first $^5D_0 \rightarrow {}^7F_1$ emission line is in fact a doublet, probably indicating a more complex structure which has not been detected for other excitations.

Therefore the dye laser selective excitation technique permits one to distinguish three types of spectra for the composition $x = 0.5$. Each of these spectra presents large linewidths characteristic of short-range disorder. The same three types of spectra are observed for $x = 0.25$ and 0.33 for which III appears only slightly.

The energy scheme in Fig. 4 represents the occurrence and evolution of the spectra for the compounds $Zr_{1-x}Ln_xO_{2-0.5x}$ in the $0.04 \leq x \leq 1$ composition range while Table IV sums up the results which can be summarized: spectrum II occurs for tetragonal zirconia ($x = 0.04$); spectra I and II occur for $0.05 \leq x \leq 0.18$; spectra I, II, and III for $0.25 \leq x \leq 0.66$; spectrum III alone for $0.75 \leq x \leq 1$ (cubic Y_2O_3 limit).

(*c*) *Discussion.* We now have to discuss what conclusions about the structure of yttria-stabilized zirconias may be extracted from our spectroscopic analysis.

The assignment of spectrum III is unambiguous. This kind of spectra has been encountered many times in Eu^{3+}-doped rare earth sesquioxides or in C-Eu_2O_3 (*27, 28*). The line wavelengths vary continuously for type-III spectrum between the compositions $Zr_{1-x}Ln_xO_{2-0.5x}$ ($x = 0.5$) and C-$Y_2O_3:Eu^{3+}$ (see Table III). This fluorescence spectrum is characteristic of Eu^{3+} in the hexacoordinated C_2-pseudo C_{2v}-sesquioxide cationic site which may be described as the center of a cube formed by six oxygens and two vacancies on a face diagonal (Fig. 5a). The other site in cubic sesquioxide (symmetry C_{3i}) is three times less numerous than C_2 and gives rise to just a few and sometimes hardly recognizable lines due to its high symmetry (*29*).

The fluorescence spectra of compositions with $x = 1$ to 0.75 are made of III alone which is natural since their only (or main) component is the C-type phase (see Table I). Spectrum III also appears (together with I and II) for $0.67 \geq x \geq 0.25$ samples characterized on the contrary by the pure fluorite F phase (with a small amount of C phase for $x = 0.67$) and this will be discussed hereafter.

TABLE III

EVOLUTION OF Eu^{3+} LINES POSITIONS FOR THE SPECTRUM III IN $Zr_{1-x}Ln_xO_{2-0.5x}$ (Ln = Y + Eu)[a]

	$x = 0.50$	$x = 0.57$	$x = 0.67$	$x = 0.75$	$x = 0.95$	$x = 1$
$^5D_0 \rightarrow {}^7F_0$	(λ_e = 5811.5)	5790	5795	5800	5805	5806
$^5D_0 \rightarrow {}^7F_1$	5885	5860	5865	5870	5875	5874.9
	5935	5930	5927	5930	5930	5930
	5965	5980	5985	5995	5995	5996
$^5D_0 \rightarrow {}^7F_2$	6115	6115	6115	6110	6110	6110.5
				6130	6130	6128.6
						6144.5
	6315	6300	6300	6300	6300	6310.9

Note. Except for $x = 0.5$ the values reported are those measured under uv broadband excitation.
[a] Comparison with Eu^{3+} in yttrium sesquioxide.

Considering now the zirconia-rich part of our system which is characterized by type-II spectrum either for the tetragonal (T) or cubic fluorite (F) crystalline form we propose to assign it to Ln^{3+} in *CN*8 (coordination number = 8) coordination for the following reasons.

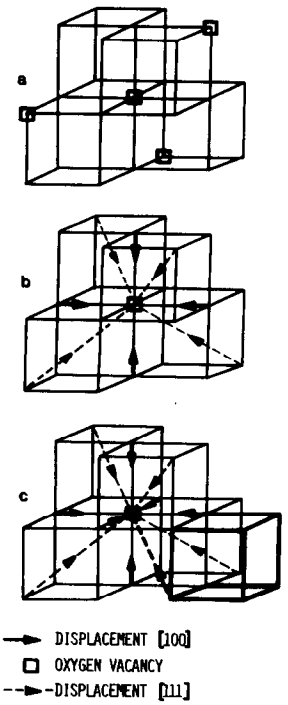

FIG. 5. (a) Ordering of vacancies in C-Ln_2O_3-type phases showing three C_2 and one C_{3i} *CN*6 cationic sites. (b) Effect of one isolated vacancy on its first-neighbor cations (4 *CN*7 sites). (c) Effect on one isolated vacancy on its 28 second-neighbor cations (28 *Cn*8 sites of *C*1 point symmetry).

An oversimplified view of the structure would lead to assign the point symmetries D_{2d} and O_h to the cationic site for T and F, respectively, by analogy with the cubic and tetragonal high-temperature pure zirconias. This is in contradiction with our spectroscopic data since we observe three lines for $^5D_0 \rightarrow {}^7F_1$ in type-II spectrum which indicates a much lower symmetry (at most C_{2v}). This fact is easily understandable by considering the effect of oxygen vacancies. On Fig. 5b is schematized a part of the fluorite unit cell. It represents four cationic positions at the center of one elementary cube out of two. The oxygen positions are the corners of each cube. One isolated oxygen vacancy then creates four sevenfold coordination cationic sites in its immediate surrounding. But as clearly demonstrated by Steele and Fender (*10*) using neutron scattering the removal of one ion causes the displacement of the nearest-neighbors oxygens following [100] axes and the secondary relaxation of oxygens in the [111] directions. These displacements of atoms from their position in the "ideal" fluorite structure in turn lower to C_1 the symmetry of cationic sites second neighbors of the va-

cancy (see Fig. 5c). In other words one vacancy creates four *CN*7 sites in its first cationic coordination shell and 28 cationic sites of *CN*8 but of symmetry C_1 in the second cationic shell. Assuming no interaction between vacancies, for the composition $x = 0.04$ we get 0.08 heptacoordinated sites for 0.92 octocoordinated of which 0.36 are O_h and 0.56 are C_1. Because at the beginning of the substitution there is much less sites of *CN*7 than sites of *CN*8 we assign the spectrum of type II to *CN*8 while the spectrum of type I, which shows up progressively with increasing concentration of lanthanides, to the occupation by europium ions of those *CN*7 sites. The spectroscopic data then tend to prove that at low Ln^3 contents the trivalent ion preferentially enters cationic sites second neighbors of oxygen vacancies. Note that the fluorescence spectrum of Eu^{3+} in true octahedral O_h symmetry has been observed, for example, in the fluorite phase $Th_{0.997}Eu_{0.003}O_{1.999}$ (*30*) and is characterized by just one magnetic dipolar $^5D_0 \rightarrow {}^7F_1$ line. So it appears that there is no occupancy by Eu^{3+} of O_h symmetry sites in stabilized zirconias.

The third spectrum (I) is also characteristic of a low symmetry (three lines are observed for $^5D_0 \rightarrow {}^7F_1$). The cationic *CN*7 sites represented on Fig. 5b are of symmetry C_{3v}. This description assumes one isolated oxygen vacancy acting with the same strength on each of the three [100] directions and on each of the four [111]. A displacement of the cation along [111] would keep the C_{3v} symmetry. In the framework of our assignment the observed lower symmetry at Ln^{3+} site shows that the relaxations repartition is not strictly isotropic. This probably indicates longer range interactions such as vacancy–vacancy, cation–vacancy, or cation–cation but with our experimental data we cannot get a more precise description of the lattice distortions.

In a previous spectroscopic study of yttria-stabilized zirconias using Er^{3+} as a local probe (Ref. (*19*)) H. Arashi states the existence of two different sites for Ln^{3+}, the first one of *CN*8 (but with a symmetry lower than O_h) the other one is not assigned by the author to a particular site symmetry (either *CN*7 or *CN*6). The relative intensity of the two corresponding spectra change continuously with x for $0.08 \leq x \leq 0.67$. In the present work we obtain similar results but we observe three different spectra attributed, respectively, to the three 8,7,6 coordinations.

On Table IV are summarized the results of the present study together with those of Steele and Fender (*10*) and with the conclusions of Shih Ming Ho (*7*) based upon chemical considerations (the sevenfold coordination bonding characteristics of Zr^{4+} ions) and electrical conductivity. The suggestion of Steele and Fender that for sufficiently high Ln^{3+} contents ($x \geq 0.24$) oxygen vacancies tend to be preferentially distributed along elementary cube-face diagonals is clearly confirmed by our observation of *CN*6 coordination for compositions $x \geq 0.25$. This in turn contradicts the description made by Shih Ming Ho of orderly Y_2O_3-stabilized zirconias which suppose the existence of Ln^{3+} (*CN*6) only for $x \geq 0.60$. As in Ref. (*10*) we assign a low (C_1) symmetry for the octocoordinated *CN*8 cationic sites but we disagree with Steele and Fender's assumption of a true C_{3v} *CN*7 site symmetry (our spectroscopic data suggest rather C_{2v} or lower site symmetry). The interpretation of Eu^{3+} fluorescence spectra does not permit a quantitative evaluation of the proportion of cations Ln^{3+} in each kind of site. So one cannot by this technique get precise information about the repartition Zr^{4+}/Ln^{3+}. All what we can say is that our results do not suggest a preferential occupancy of (CN7) vacancy first-neighbor sites by Ln^{3+} but rather would lead to the

TABLE IV

SUMMARY OF RESULT COMPARISON WITH THOSE DEDUCED FROM REFS. (*7*, *10*)

	From Shih Ming Ho (Ref. (*7*))						This work		From Steele and Fender (Ref. (*10*))
	Number of Y^{3+}			Number of Zr^{4+}		Hypothetical fluorescence spectra	Observed fluorescence spectra	Observed X-ray diffraction	Conclusions and hypothetical fluorescence spectra
	*CN*8	*CN*7	*CN*6	*CN*8	*CN*7				
$Zr_{0.96}Ln_{0.04}O_{1.98}$							II(+ monoclinic)	T(+ M)	
$Zr_{0.95}Ln_{0.05}O_{1.975}$							I + II	T(+ M)	$Zr_{0.82}Ln_{0.18}O_{1.91}$ and $Zr_{0.78}Ln_{0.22}O_{1.89}$:
$Zr_{0.90}Ln_{0.10}O_{1.95}$							I + II	T	relaxations toward oxygen vacancies
$Zr_{0.84}Ln_{0.16}O_{1.92}$	0.16	—	—	0.52	0.32	II			*CN* = 8 symmetry C_1 (II spectrum)
$Zr_{0.82}Ln_{0.18}O_{1.91}$							I + II	F	*CN* = 7 symmetry C_{3v} (not observed)
$Zr_{0.80}Ln_{0.20}O_{1.90}$	0.20	—	—	0.40	0.40	II			
$Zr_{0.75}Ln_{0.25}O_{1.875}$							I + II + III	F	Tendency for associations $Ln^{3+}(CN7)$–vacancy–$Ln^{3+}(Cn7)$
$Zr_{0.68}Ln_{0.32}O_{1.84}$	0.32	—	—	0.04	0.64	II			
$Zr_{0.67}Ln_{0.33}O_{1.835}$							I + II + III	F	$Zr_{0.76}Ln_{0.24}O_{1.87}$ tendency for *CN* = 6 site (III spectrum)
$Zr_{0.64}Ln_{0.36}O_{1.82}$	0.28	0.08	—	—	0.64	I + II	I + II + III	F	
$Zr_{0.50}Ln_{0.50}O_{1.75}$	—	0.50	—	—	0.50	I	I + II + III	F	
$Zr_{0.43}Ln_{0.57}O_{1.715}$							I + II + III	F	
$Zr_{0.40}Ln_{0.60}O_{1.70}$	—	0.40	0.20	—	0.40	I + III			
$Zr_{0.33}Ln_{0.67}O_{1.665}$							I + II + III	F(+ C)	
$Zr_{0.25}Ln_{0.75}O_{1.624}$	—	0.25	0.50	—	0.25	I + III	III	(F) + C	
$Zr_{0.18}Ln_{0.82}O_{1.59}$							III	(F) + C	
$Zr_{0.11}Ln_{0.89}O_{1.555}$							III	C	
$Zr_{0.05}Ln_{0.95}O_{1.525}$							III	C	
$Zr_{0.01}Ln_{0.99}O_{1.505}$							III	C	

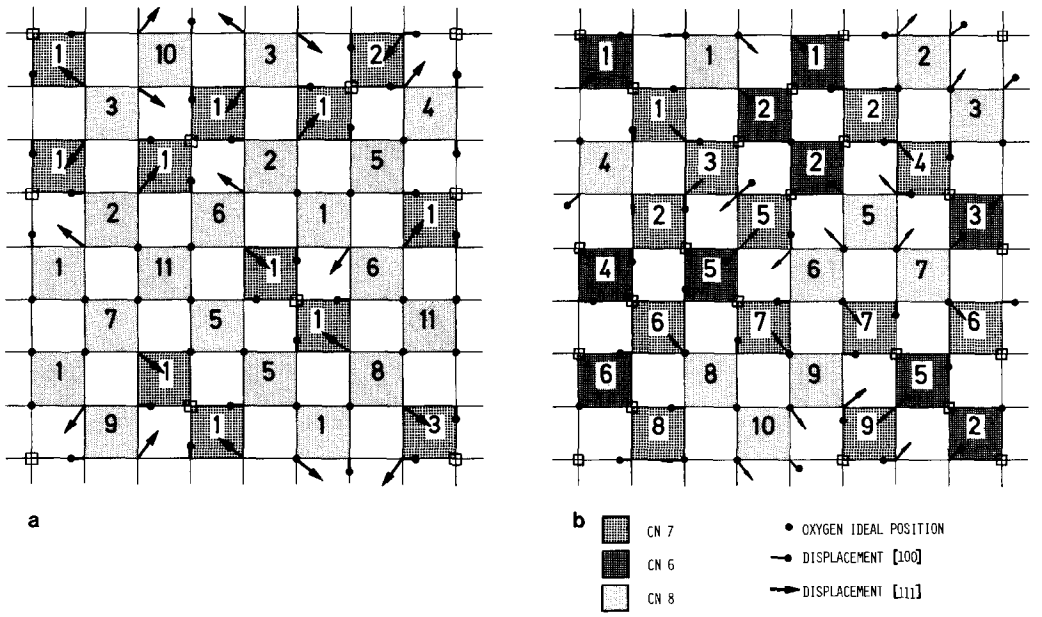

FIG. 6. (a) Model for $Me\ O_{1.906}$. (b) Model for $MeO_{1.75}$. In each *CN* different numbers correspond to different cationic sites.

inverse conclusion at least for very low trivalent ion contents ($x = 0.04$) for which Ln^{3+} (*CN*8) is the only species identified.

The last point we want to discuss is the large "glassy like" linewidths of Eu^{3+} fluorescence in yttria-stabilized zirconia, a characteristic that was also observed for the single crystal ($x = 0.25$) sample. X-Ray diffraction proves that cations are on a cfc lattice without long-range ordering between Zr^{4+} and Ln^{3+}. The cause of the "glassy like" structure has then to be searched for in the (oxygen ion + vacancies) arrangement toward cationic positions. We have already described the effect of one isolated vacancy on its first and second neighbors. When vacancies proportion increases (with x) their relative disposition acts on the cationic sites directly by creating hexacoordinated (*CN*6) sites and indirectly by means of ion relaxations. On Fig. 6 we have schematized in a very simple manner these effects in order to evaluate how much the local structure may be disordered even for relatively low vacancy concentrations. Figure 6a corresponds to the composition $Zr_{0.812}Ln_{0.188}O_{1.906}$. It represents the (001) plane with oxygen atoms at the corners of each little square. Cations are located at $a/4$ (where a is the cell parameter) above one square out of two. To simplify the drawing the $a/2$ oxygen plane is supposed completely filled whereas all the vacancies are in the basic plane which then contains six vacancies over the 64 anionic positions. Vacancies are distributed so as to create only *CN*8 and *CN*7 cationic sites according to our spectroscopic assignments. The oxygen displacements are represented by arrows along [100] and along the projection of [111]. One can see that even by considering only the first-coordination shells we have created a large number of different immediate environments around cations. For the particular solution depicted on Fig. 6a one may count three *CN*7 point sites and eleven *CN*8 differing in each case by the ligands relative positions. The number of different

point sites still increases with the number of vacancies. On Fig. 6b, for example, we have schematized the $Zr_{0.5}Ln_{0.5}O_{1.75}$ composition by applying the same rules as above except that hexacoordinated sites are now considered. One can identify on this diagram nine different *CN*8 sites, eight different *CN*7, and five different *CN*6. These representations are only two among the equivalent solutions one could imagine. Nevertheless they clearly show that the simple consideration of relaxations toward oxygen vacancies creates a large number of sites for the cations and this for each value of the coordination number. The Eu^{3+} optically active cations then experience a great number of slightly different surroundings—just as in a glass—which causes the fluorescence lines unhomogeneous broadening.

IV. Conclusion

The study of so-called yttria-stabilized zirconias ($Zr_{1-x}Y_xO_{2-0.5x}$) by means of the optically active Eu^{3+} local probe partially substituting Y^{3+} has been made over a wide range of compositions. The interpretation of europium fluorescence spectra observed either under ultraviolet excitation or under dye laser selective excitation leads to several interesting conclusions about the structure of the cationic and mainly the anionic sublattices that could not be reached by macroscopic investigation techniques. The main conclusions of this work are the following.

The stabilization process which we have observed for samples containing at least 4% trivalent cations ($x = 0.04$) is accompanied by a drastic change in the cation's immediate surroundings by comparison with monoclinic nonstabilized zirconia (see Ref. (*27*)). On the other hand the phase transformations from tetragonal to cubic (fluorite) to cubic (C-type)-stabilized zirconias bring no change in Eu^{3+} fluorescence other than the continuous evolution observed for $0.04 \leq x \leq 1$. Over this composition range our results are consistently interpreted by a model in which cations are surrounded by 8, 7, or 6 oxygen first-neighbors. When x increases we observe successively *CN*8, *CN*8 + *CN*7, *CN*8 + *CN*7 + *CN*6 coordinations. The site symmetry may be C_1, C_s, C_2, D_2, or C_{2v} for *CN*8 and *CN*7. It is C_2(pseudo C_{2v}) for *CN*6, the two oxygen vacancies being on a face diagonal. There is no indication of a preferential repartition of oxygen vacancies immediately near the heterovalent Ln^{3+} cations. This last point may nevertheless be discussed since fluorescence spectra do not give information about the number of ions in each site. The low symmetry which is observed for *CN*8 directly proves that the remaining oxygen atoms are relaxed toward oxygen vacancies. For *CN*7 sites the simple consideration of relaxations towards an isolated vacancy lead to C_{3v} symmetry. Lower symmetry is explainable only by longer range ion–ion or ion–vacancy interactions. Finally, the common characteristic of Eu^{3+} in stabilized zirconias—i.e., the fluorescence lines unhomogeneous broadening—is another evidence for the various relaxations occurring in the oxygen lattice leading to a large number of slightly different sites for each coordination number.

In summary, in view of our structural analysis by means of the Eu^{3+} local probe, the yttria-stabilized zirconias may well be described by a cfc cationic sublattice in which trivalent and tetravalent cations are statistically distributed. The anionic sublattice accommodates vacancies at random on oxygen positions. These vacancies in turn cause complex oxygen displacements giving rise to what we may describe as a "glass" of anions.

References

1. P. Duwez, F. H. Brown, and F. Odell, *J. Electrochem. Soc.* **98**, 356 (1951).

2. B. V. NARASIMHA RAO AND T. P. SCHREIBER, Communication of the American Ceramic Society, C-44 (March 1982).
3. T. H. ETSELL AND S. N. FLENGAS, *Chem. Rev.* **70,** 339 (1970).
4. T. H. ETSELL AND S. N. FLENGAS, *Metall. Trans.* **3,** 27 (1972).
5. M. FAUCHER, K. DEMBINSKY, AND A. M. ANTHONY, *Amer. Ceram. Soc. Bull.* **49,** 707 (1970).
6. E. GREENBERG, G. KATZ, R. REISFELD, N. SPECTOR, R. C. MARSHALL, B. BENDON, AND R. L. BROWN, *J. Chem. Phys.* **77,** 4797 (1982).
7. SHIH MING HO, *Mater. Sci. Eng.* **54,** 23 (1982).
8. P. ABELARD AND J. F. BAUMARD, *Phys. Rev. B* **26,** 1005 (1982).
9. V. BUDTLER, C. R. A. CATLOW, AND B. E. F. FENDER, *Solid State Ionics* **5,** 539 (1981).
10. D. STEELE AND B. E. F. FENDER, *J. Phys. C* **7,** 1 (1974).
11. H. G. SCOTT, *J. Mater. Sci.* **10,** 1527 (1975); **12,** 311 (1977).
12. S. P. RAY AND V. S. STUBICAN, *Mater. Res. Bull.* **12,** 549 (1977); **15,** 1419 (1980); V. S. STUBICAN, R. C. HINK, AND S. P. RAY, *J. Amer. Chem. Soc.* **61,** 17 (1978).
13. C. PASCUAL AND P. DURAN, *Amer. Ceram. Soc.* **66,** 23 (1983).
14. J. DEXPERT-GHYS, M. FAUCHER, AND P. CARO, *J. Solid State Chem.* **41,** 27 (1982); *Phys. Rev. B* **23,** 2 (1981).
15. R. J. HAMERS, J. R. WIETFELDT, AND J. C. WRIGHT, *J. Chem. Phys.* **77,** 683 (1982).
16. L. C. PORTER AND J. C. WRIGHT, *J. Chem. Phys.* **77,** 2322 (1982).
17. C. BRECHER AND L. A. RISEBERG, *Phys. Rev. B* **13,** 81 (1976).
18. J. S. THORP, A. AYPAR, AND J. S. ROSS, *J. Mater. Sci.* **7,** 729 (1972).
19. H. ARASHI, *Phys. Status Solidi A* **10,** 107 (1972).
20. E. ANTIC, M. LEMAITRE-BLAISE, P. CARO, AND J. P. COUTURES, *High-Temp. Press.* **8,** 585 (1976).
21. T. K. GUPTA, J. H. BECHTOLD, R. C. KUZNICKI, L. H. CADOFF, AND B. R. ROSSING, *J. Mater. Sci.* **12,** 2421 (1977).
22. K. K. SRIVASTAVA, R. N. PATIL, C. B. CHOUDARY, K. V. G. K. GOKHALE, AND E. C. SUBBA RAO, *Trans. J. Brit. Ceram. Soc.* **73,** 85 (1974).
23. J. DEXPERT-GHYS, M. FAUCHER, H. DEXPERT, AND P. CARO, *J. Phys. (Orsay, Fr.)* **12,** C7–95 (1977).
24. M. J. WEBER, J. A. PAISNER, S. S. SUSSMAN, W. M. YEN, L. A. RISEBERG, AND C. BRECHER, *J. Lumin.* **12/13,** 729 (1976).
25. P. AVOURIS, A. CAMPION, AND M. A. EL-SAYED, *J. Chem. Phys.* **67,** 3397 (1977).
26. M. J. WEBER, *in* "Laser Spectroscopy of Solids" (W. M. Yen and P. M. Selzer, Eds.), p. 189–239, Springer-Verlag, Berlin/Heidelberg/New York (1981).
27. J. DEXPERT-GHYS, M. FAUCHER, AND P. CARO, *C.R.A.S., Paris* **298**(II), 621 (1984).
28. J. DEXPERT-GHYS AND M. FAUCHER, *Phys. Rev. B* **20,** 10 (1979).
29. P. TOLA, J. DEXPERT-GHYS, M. LEMONNIER, A. RETOURNARD, M. PAGEL, AND J. GOULON, *Chem. Phys.* **78,** 339 (1983).
30. J. DEXPERT-GHYS, Thèse de Doctorat d'Etat Paris, Sud Orsay, France (1979).